

## ON THE STABILITY OF LOOSE AND STRONG PARTITIONED ALGORITHMS FOR THERMAL COUPLING OF DOMAINS USING HIGHER ORDER IMPLICIT TIME INTEGRATION SCHEMES

V. Kazemi-Kamyab\*, A.H. van Zuijlen, H. Bijl

Aerodynamics Section, Faculty of Aerospace Engineering, Delft University of Technology  
P.O. Box 5058, 2600 GB Delft, The Netherlands.

\* (v.kazemikamyab@tudelft.nl)

### Abstract.

*Thermal interaction of fluids and solids, or conjugate heat transfer (CHT), is encountered in many engineering applications. Since time-accurate computations of such coupled problems can be computationally expensive, we consider loosely-coupled and strongly-coupled solution algorithms in which higher order multi-stage Runge-Kutta schemes are employed for time integration. The higher order time integration schemes have the potential to improve the computational efficiency at arriving at a certain accuracy relative to the traditionally used 1<sup>st</sup> and 2<sup>nd</sup> order implicit schemes. The spatial coupling between the subdomains is realized using Dirichlet-Neumann interface conditions and the coupled domains are solved in a sequential manner at each stage (Block Gauss-Seidel). In this paper, the stability of two partitioned algorithms is analyzed by considering a one dimensional model problem. The model problem consists of two thermally coupled domains where the governing equation within each subdomain is unsteady linear heat conduction.*

*In the loosely-coupled approach, a family of multi-stage IMEX schemes is used for time integration. By observing similarities between the second stage of the IMEX schemes and the  $\theta$  scheme with  $\theta = 0.5$  (Crank-Nicolson), the stability of the partitioned algorithm in which the Crank-Nicolson scheme is used for time integration is first analyzed by applying the stability theory of Godunov-Ryabenkii. The stability of the IMEX schemes is next investigated by numerically solving the model problem and comparing the results to the conclusions of the stability analysis for the Crank-Nicolson scheme. Due to partly explicit nature of the IMEX schemes, the loosely-coupled algorithm becomes unstable for sufficiently large Fourier numbers (similar to the Crank-Nicolson scheme). When the ratio of the thermal effusivities of the coupled domains is much smaller than unity, time step restriction due to stability is sufficiently weak that computations can be performed with reasonably large Fourier numbers. Furthermore, the results show better stability properties of the IMEX schemes compared to the Crank-Nicolson scheme.*

*In the strongly-coupled approach, the stability and rate of convergence of performing (Gauss-Seidel) subiterations at each stage of the higher order implicit ESDIRK time integration schemes are analyzed. From the stability analysis, an expression for the rate of convergence of the iterations ( $\sigma$ ) is obtained. For cases where  $\sigma \ll 1$ , subiterations will converge*

rapidly. However, when  $\sigma \approx 1$ , the convergence rate of the iterations is slow. The results obtained by solving the model problem numerically are in line with the performed analytical stability analysis.

**Keywords:** *High order implicit time integration, Conjugate heat, Partitioned algorithm, Stability.*

## 1. INTRODUCTION

Thermal interaction of flows and structures, also referred to as conjugate heat transfer, arises in many engineering applications. Numerical simulations help to obtain a better understanding of the physics of the coupled problem and hence to increase the efficiency and/or safety of designs.

In order to take advantage of the already existing efficient and highly optimized separate fluid and solid codes, the coupled problem needs to be solved in a partitioned manner. In the partitioned method, the domain is decomposed into sub-domains and separate fluid and solid codes are used for solving the temperature field within their respective regions. Any two subdomains are coupled through a set of transmission conditions at the interface (to ensure that the interface equations are satisfied) where one transmission condition is assigned to one side and the other to the opposite side of the interface [1]. Therefore, in the partitioned approach, the interface equations are solved in a weakly coupled or segregated manner [1].

To advance the coupled problem in time, implicit time integrations are considered in order to circumvent time step restrictions due to probable stiffness in the problem. In the partitioned method, with implicit time integration, some or all of the interface terms are treated explicitly, depending on the arrangement with which the two coupled domains are solved (parallel (Block Jacobi) or sequential (Block Gauss-Seidel)). If at each time-step, a single implicit solve of each of the solvers is performed, the partitioned algorithm is referred to as loosely-coupled, and otherwise it is referred to as strongly-coupled.

In the literature, for numerical solution of unsteady CHT problems, loosely-coupled and strongly-coupled solution algorithms with up to second order implicit time integration schemes have been reported. Since time-accurate computations of such coupled problems can be computationally expensive, we consider loosely-coupled and strongly-coupled solution algorithms in which higher order multi-stage Runge-Kutta schemes are employed for time integration. The higher order time integration schemes have the potential to improve the computational efficiency at arriving at a certain accuracy relative to the traditionally used 1<sup>st</sup> and 2<sup>nd</sup> order implicit schemes [2]. The spatial coupling between the subdomains is realized using Dirichlet-Neumann interface conditions and the coupled domains are solved in a sequential manner at each stage (Block Gauss-Seidel). In this paper, the stability of two partitioned algorithms is analyzed by considering a one dimensional model problem. The model problem consists of two thermally coupled domains where the governing equation within each subdomain is unsteady linear heat conduction.

In the loosely-coupled approach a family of higher order multi-stage mixed implicit-explicit (IMEX) Runge-Kutta schemes is used for time integration. The higher order IMEX schemes consist of the ESDIRK schemes for implicit integration of the spatially discretized

governing equations within each subdomain and equal order and number of stages ERK schemes for explicit integration of all or part of the coupling terms. For the partitioned solution of the mechanical coupling of flows and structures, van Zuijlen and Bijl [2] demonstrated the temporal order preservation of the IMEX schemes without the need to perform subiterations and their computational efficiency relative to the second order Backward Differencing scheme (*BDF2*). By noting similarities between the second stage of the IMEX schemes and the  $\theta$  scheme with  $\theta = 0.5$  (Crank-Nicolson), the stability of the partitioned algorithm in which the Crank-Nicolson scheme is used for time integration is first analyzed. Following Giles [3] (in which the stability of a loosely-coupled algorithm with Backward Euler for time integration was analyzed), the stability theory of Godunov-Ryabenkii is used to perform the stability analysis. The stability of the IMEX schemes is next investigated by numerically solving the model problem and comparing the results to the conclusions of the stability analysis for the Crank-Nicolson scheme.

In the strongly-coupled approach, the stability and rate of convergence of performing (Gauss-Seidel) subiterations at each stage of the higher order implicit ESDIRK time integration schemes are analyzed following the stability analysis in Henshaw and Chand [1] (in which the  $\theta$  scheme is used for time integration). From the stability analysis, an expression for the rate of convergence of the iterations is obtained. By solving the model problem numerically, the results are compared to the performed analytical stability analysis.

In what follows we first give a description of the one dimensional model problem. Next, the semi-discrete form of the coupled problem is obtained by discretizing the coupled domains in space using vertex-centered finite volume method. This is followed by a brief overview of the ESDIRK and IMEX time integration schemes. Next, the stability of loosely-coupled and strongly-coupled partitioned algorithms in which the higher order Runge-Kutta schemes are used for time integration is analyzed using the one dimensional model problem.

## 2. MODEL PROBLEM

In this section, the description of the model problem used for analyzing the stability of the partitioned algorithms is presented. The one dimensional model problem consists of thermal coupling of two domains  $\Omega_1 = [-L_1, 0]$  and  $\Omega_2 = [0, L_2]$  which are separated by the interface  $\mathcal{I}$  at  $x = 0$ . The governing equation within each sub-domain is transient linear heat conduction. The boundary-value problem is given by:

$$(\rho c_p)_m \frac{\partial T_m(x, t)}{\partial t} = - \frac{\partial q_m(x, t)}{\partial x}, \quad \text{for } x \in \Omega_m, m = 1, 2 \quad (1)$$

$$q_m(x, t) = -k_m \frac{\partial T_m(x, t)}{\partial x}, \quad \text{for } x \in \Omega_m, m = 1, 2 \quad (2)$$

where  $T_m$  and  $q_m$  represent the temperature and heat flux fields within each domain respectively with  $m$  the index of the subdomain. For simplicity, each sub-domain has homogenous material properties (constant  $k$  thermal conductivity,  $c_p$  heat capacity, and  $\rho$  density). The

initial and boundary conditions are:

$$T_2(\mathcal{I}, t) = T_1(\mathcal{I}, t), \quad (3)$$

$$k_1 \frac{\partial T_1(x, t)}{\partial x} \Big|_{\mathcal{I}} = k_2 \frac{\partial T_2(x, t)}{\partial x} \Big|_{\mathcal{I}}, \quad (4)$$

$$T_1(-L_1) = T_{1,lb}, \quad T_2(L_2) = T_{2,rb}, \quad (5)$$

$$T_m(x, t = 0) = T_m^o(x) \quad \text{for } x \in \Omega_m, m = 1, 2. \quad (6)$$

The non-interface boundaries (5) are constant Dirichlet conditions. To couple the solution of the subdomains at the interface, as (3) and (4) show, the Dirichlet-Neumann interface conditions are considered. For partitioned algorithms, the stability of the coupling algorithm depends on the correct assignment of the interface conditions. Using a similar model problem, Henshaw and Chand [1] analyzed the stability and rate of convergence of interface iterations for Dirichlet-Neumann interface conditions without any particular assumption on the spatial discretization, with the  $\theta$  scheme for time integration. The following estimate for the rate of convergence of the iterations was obtained:

$$\sigma_{est} \approx \frac{k_2}{k_1} \sqrt{\frac{\alpha_1}{\alpha_2}}, \quad (7)$$

with  $\alpha_m = \left(\frac{k}{\rho c_p}\right)_m$  representing the thermal diffusivity of each subdomain. The estimate was obtained by imposing the Dirichlet (temperature) condition on  $\Omega_2$  and the Neumann (the heat flux) condition on  $\Omega_1$ . Performing interface iterations based on the assigned interface boundary conditions will provide a stable solution if  $\sigma_{est} < 1$ , otherwise the two interface boundary conditions must be interchanged. While this estimate has been obtained for a strongly-coupled solution algorithm, it can also be used as a criterion for imposing interface boundary conditions for loosely-coupled solution algorithms; that is, for stability of a loosely-coupled partitioned algorithm satisfying (7) is necessary but might not be sufficient. Here, it is assumed that based on the material properties of the two subdomains, the imposed interface boundary conditions satisfy the criterion (7), i.e. the temperature condition is assigned to  $\Omega_2$  and the heat flux condition to  $\Omega_1$ .

Furthermore, noting that the thermal effusivity of a material is given by  $e = \frac{k_m}{\sqrt{\alpha_m}} = \sqrt{k_m \rho_m c_{p,m}}$ ,  $\sigma_{est}$  in (7) is equal to the ratio of the thermal effusivities of the coupled domains ( $\sigma_{est} = \frac{e_2}{e_1}$ ).

When analyzing the stability of the loosely-coupled solution algorithm, the two coupled domains are considered as semi-infinite. The non-interface boundary conditions ( $x \rightarrow \pm\infty$ ) are then given by  $T_1(x \rightarrow -\infty) = T_{1,lb}$  and  $T_2(x \rightarrow \infty) = T_{2,rb}$ .

### 3. SEMI-DISCRETIZED FORM OF THE COUPLED PROBLEM

The method of lines is used to solve the coupled PDE (space and time discretizations are carried out separately), with space being discretized first to obtain the semi-discrete form of the coupled problem. The two domains are discretized in space using vertex-centered finite volume (VVF) method (see Fig.1).

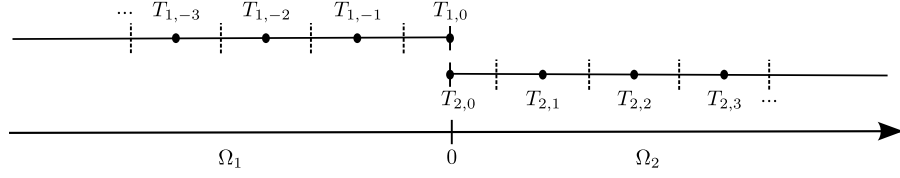


Figure 1. Discretization of  $\Omega_1$  and  $\Omega_2$  subdomains using FVF.

Applying the volume integral form of the governing equation (1) to each control volume results in:

$$(\Delta x \rho c_p)_m \frac{d}{dt} T_{m,j} = -q_m|_{j-1/2}^{j+1/2} \quad m = 1, 2, \quad (8)$$

where for simplicity cells of equal size are used within each subdomain (for the interface cell,  $T_{1,0}$ ,  $\Delta x_1$  is replaced with  $\frac{\Delta x_1}{2}$ ).

Substituting (2) for  $q_m$  into (8) and using central difference to approximate the temperature gradients at the cell faces, the semi-discrete form of equation (1), for the interior cells, with some rearrangements is given by:

$$(\Delta x \rho c_p)_m \frac{d}{dt} T_{m,j} = \frac{k_m}{\Delta x_m} T_{m,j+1} - \frac{2k_m}{\Delta x_m} T_{m,j} + \frac{k_m}{\Delta x_m} T_{m,j-1} = \mathcal{F}_{m,j} \quad m = 1, 2, \quad (9)$$

where  $\mathcal{F}_{m,j}$  is the cell-residual obtained as a result of discretizing the governing equation in space.

The semi-discrete form of  $T_{2,1}$  is also given by (9) where the value of the interface temperature  $T_{2,\mathcal{I}} = T_{2,0}$  is obtained by prescribing the temperature of the interface node in  $\Omega_1$  as its value, i.e.  $T_{2,0} = T_{1,0}$ .

In  $\Omega_1$ , the discretization of  $T_{1,0}$  is given by:

$$\left(\frac{\Delta x}{2} \rho c_p\right)_1 \frac{d}{dt} T_{1,0} = -q_{1,0} - \frac{k_1}{\Delta x_1} (T_{1,0} - T_{1,-1}) = \mathcal{F}_{1,0}, \quad (10)$$

where  $q_{1,\mathcal{I}} = q_{1,0}$  is obtained by prescribing  $q_{2,0}$  as its value:

$$q_{1,0} = q_{2,0} = -\frac{k_2}{\Delta x_2} (T_{2,1} - T_{2,0}). \quad (11)$$

The semi-discrete form of the coupled problem can be expressed by the following two coupled ODE systems:

$$M_1 \frac{d}{dt} \mathbf{T}_1 = \mathcal{F}_1(\mathbf{T}_1, q_{\mathcal{I}}, t), \quad (12)$$

$$M_2 \frac{d}{dt} \mathbf{T}_2 = \mathcal{F}_2(\mathbf{T}_2, T_{\mathcal{I}}, t), \quad (13)$$

where  $\mathbf{T}_1$  and  $\mathbf{T}_2$  are vectors containing the discrete solution in the FV cells,  $M_1$  and  $M_2$  are diagonal matrices containing the product of the cells' volumetric heat capacities  $((\rho c_p)_{m,j})$  with the cell volumes, and  $\mathcal{F}_1$  and  $\mathcal{F}_2$  are the residual vectors. The coupling between the two systems is through the interface temperature  $T_{\mathcal{I}}$  and heat flux  $q_{\mathcal{I}}$ .

#### 4. TIME INTEGRATION

In this paper a family of multi-stage implicit Runge-Kutta schemes (IRK), namely the Explicit first stage, Singly Diagonally Implicit Runge-Kutta (ESDIRK) schemes, is considered for time integration which can be made of arbitrary higher orders while retaining the L-stability property. For a coupled ODE system of the form  $M \frac{d\mathbf{T}}{dt} = \mathcal{F}(\mathbf{T}, t)$ , the solution at each stage of the ESDIRK scheme can be written as:

$$M\mathbf{T}^{(k)} = M\mathbf{T}^n + \Delta t \sum_{i=1}^k a_{ki}^I \mathcal{F}(t^n + c_i \Delta t, \mathbf{T}^{(i)}) = M\mathbf{T}^n + \Delta t \sum_{i=1}^k a_{ki}^I \mathcal{F}^{(i)}, \quad (14)$$

where  $a_{ki}^I$  are the coefficients of the corresponding stage and  $c_i = \sum_j a_{ij}^I$  is the location (quadrature node) of the stage solution at  $t^{(i)} = t^n + c_i \Delta t$ . High order solution at the next time level can be achieved by the weighted sum of the stage residuals such that the lower order errors cancel out:

$$\mathbf{T}^{n+1} = \mathbf{T}^n + M^{-1} \Delta t \sum_{i=1}^s b_i \mathcal{F}^{(i)}, \quad (15)$$

where  $b_i$  are the weight factors with  $\sum_i b_i = 1$ , and  $s$  is the number of stages. In this paper, stiffly accurate ESDIRK schemes are considered where  $a_{si}^I = b_i$  and thus the solution of the last stage is equal to the solution of the time-level,  $\mathbf{T}^{n+1} = \mathbf{T}^s$ . Therefore when a fully coupled approach is used to solve the coupled problem, computing (15) is not necessary. The coefficients and weights are usually arranged in Butcher tableau (see Table 1). For the ESDIRK schemes, as the name implies, the diagonal coefficients are equal ( $a_{kk} = \gamma$ ).

In solving time-accurate advection-diffusion-reaction problems, where separable stiff and non-stiff components are identifiable, Kennedy and Carpenter [4] present a family of higher order implicit ESDIRK schemes to integrate the stiff components of the problem (to retain stability) and a family of higher order explicit ERK schemes (which are computationally less expensive than the corresponding implicit schemes) to integrate the non-stiff components of the problem. The resultant family of time integration schemes which is a combination of implicit and explicit time integration schemes is denoted by mixed implicit-explicit (IMEX) schemes. In this paper, the coefficients of the implicit ESDIRK schemes are denoted by  $a_{ki}^I$  and that of the ERK schemes by  $a_{ki}^E$  as shown in Table 1. In order to be consistent with the ESDIRK schemes, the introduced ERK schemes have the same weight factors  $b_i$  and  $c_i$  coefficients as the ESDIRK schemes. The presented higher order multi-stage IMEX schemes in [4] are an example of additive RK schemes; while the temporal order of accuracy of each stage is low order, here second order, by using (15) to evaluate the solution to the time-level, the truncation errors of the stages cancel such that the time-level solution has the designed higher order accuracy.

Analogously and following [2] (where the mechanical coupling of fluids and structures is considered), for loosely-coupled solution of the coupled problem, the higher order IMEX schemes presented in [4] are used to advance the solution to the coupled problem in time; the ESDIRK schemes are used for implicit integration of the spatially discretized governing equations within the coupled domains and equal order and equal number of stages ERK schemes are used for explicit integration of all or part of the coupling terms (depending on whether Block Jacobi or Block Gauss-Seidel is used to solve the coupled problem at each stage).

By expressing the predictor-corrector  $\theta$  scheme, used in [5] for solving unsteady CHT problems, in terms of a two-stage IMEX scheme (its butcher tableau is given in Table 2),

$c_1$	0	0	0	0	$c_1$	0	0	0	0
$c_2$	$a_{21}^I$	$a_{22}^I$	0	0	$c_2$	$a_{21}^E$	0	0	0
$c_3$	$a_{31}^I$	$a_{32}^I$	$a_{33}^I$	0	$c_3$	$a_{31}^E$	$a_{32}^E$	0	0
$c_4$	$a_{41}^I$	$a_{42}^I$	$a_{43}^I$	$a_{44}^I$	$c_4$	$a_{41}^E$	$a_{42}^E$	$a_{43}^E$	0
	$b_1$	$b_2$	$b_3$	$b_4$		$b_1$	$b_2$	$b_3$	$b_4$

Table 1. A four stage additive RK method consisting of an ESDIRK and ERK scheme.

similarities can be observed between the  $\theta$  scheme with  $\theta = 0.5$  (Crank-Nicolson) and the second stage of the higher order IMEX schemes. For the second stage of the IMEX schemes, the coefficients of the corresponding ESDIRK and ERK schemes are respectively given by  $a_{21}^I = \gamma$ ,  $a_{22}^I = \gamma$ , and  $a_{21}^E = 2\gamma$  and those of the (predictor-corrector) Crank-Nicolson scheme are  $a_{21}^I = 0.5$ ,  $a_{22}^I = 0.5$ ,  $a_{21}^E = 1$ .

0	0	0	$c_1$	0	0
1	$\theta$	$1 - \theta$	$c_2$	1	0
	$\theta$	$1 - \theta$		$\theta$	$1 - \theta$

Table 2. Butcher tableau for the predictor-corrector  $\theta$  scheme.

In the partitioned approach using an implicit time integration scheme, as a result of the segregated treatment of the interface equations, the partitioned solution contains an additional source of error, compared to the monolithic solution, denoted as the partitioning error,  $\epsilon(x, t)$ . Therefore, there is the possibility of numerical instability not inherent in the monolithic approach [3]. In what follows, we analyze and investigate the stability of the (loosely-coupled and strongly-coupled) partitioned algorithms in which the coupled problem is advanced in time using the higher order time integration schemes.

Noting that the higher order IMEX schemes consist of implicit Runge-Kutta stages, it is not straight forward to apply the stability theory of Godunov and Ryabenkii to study the stability properties of the resultant loosely-coupled algorithm. However, based on the observation regarding the similarities between the second stage of the IMEX schemes and the Crank-Nicolson scheme, we will proceed with first performing stability analysis for the loosely-coupled partitioned algorithm in which the  $\theta$  scheme is used for time integration. The stability of the IMEX schemes is next investigated by considering some numerical experiments and the results are compared to the conclusions of the stability analysis for the Crank-Nicolson scheme. We wish to examine if similarities can be observed regarding the stability of the two time integration schemes and thus providing some guidelines for CHT problems where the IMEX schemes are suited for.

## 5. STABILITY ANALYSIS OF $\theta$ SCHEME

In this section, the stability of the loosely-coupled solution algorithm in which the predictor-corrector  $\theta$  scheme is used for time integration is analyzed. Of particular interest, is the stability of the algorithm when  $\theta = 0.5$  (Crank-Nicolson). Following Giles [3], the stability theory of Godunov and Ryabenkii is used to analyze the stability of this partitioned algorithm. In order to simplify the analysis, the explicit corrector step will not be incorporated into the stability analysis. In the results section, the stability of the algorithm, with the explicit

corrector step included, is investigated numerically. The full details of the stability analysis is presented in [5].

The one-dimensional model problem used for the stability analysis consists of thermal coupling of two semi-infinite domains (see Section 2 for the description). The domains are discretized in space using the vertex-centered finite volume method. By applying the  $\theta$  scheme to the semi-discrete form of the problem, the following system of equations for the loosely-coupled partitioned algorithm with integrating  $\Omega_1$  first (BGS-12) is obtained:

$$\begin{aligned}
T_{1,j}^{n+1} &= T_{1,j}^n + \theta d_1(T_{1,j-1} - 2T_{1,j} + T_{1,j+1})^{n+1} \\
&\quad + (1 - \theta)d_1(T_{1,j-1} - 2T_{1,j} + T_{1,j+1})^n \quad j < 0, \\
T_{1,0}^{n+1} &= T_{1,0}^n - 2\theta d_1(T_{1,0} - T_{1,-1})^{n+1} \\
&\quad - 2(1 - \theta)d_1(T_{1,0} - T_{1,-1})^n + 2rd_2(T_{2,1} - T_{2,0})^n \quad m = 1, j = 0, \\
T_{2,j}^{n+1} &= T_{2,j}^n + \theta d_2(T_{2,j-1} - 2T_{2,j} + T_{2,j+1})^{n+1} \\
&\quad + (1 - \theta)d_2(T_{2,j-1} - 2T_{2,j} + T_{2,j+1})^n \quad j > 0, \\
T_{2,0}^{n+1} &= T_{1,0}^{n+1}, \\
T_{2,0}^n &= T_{1,0}^n,
\end{aligned} \tag{16}$$

where  $r$  is defined by:

$$r = \frac{(\rho c_p \Delta x)_2}{(\rho c_p \Delta x)_1}, \tag{17}$$

and  $d_m$  (the Fourier number of  $\Omega_m$ ) by:

$$d_m = \frac{\Delta t k_m}{(\rho c_p)_m \Delta x_m^2} = \frac{\Delta t \alpha_m}{\Delta x_m^2}. \tag{18}$$

Noting that BGS-12 is used to solve the coupled problem,  $T_{2,0}^{n+1} = T_{1,0}^{n+1}$  and  $T_{2,0}^n = T_{1,0}^n$ . In the discretization of  $T_{1,0}^{n+1}$ , the interface heat flux at  $t^{n+1}$ ,  $q_{1,0}^{n+1}$ , is predicted using its previous time step solution ( $q_{1,0}^* = q_{1,0}^n$ ). Following Giles [3], the stability of the loosely-coupled partitioned algorithm is analyzed by expressing the form of the solution using normal modes. For this partitioned algorithm, the form of the normal mode solution is given by:

$$T_{m,j}^n = z^n \kappa_m^j = \begin{cases} z^n \kappa_1^j & m = 1, j \leq 0, \\ z^n \kappa_2^j & m = 2, j \geq 0 \end{cases} \tag{19}$$

where the two last equations in (16) are satisfied as a result of the selected normal modes. Substituting the form of the normal mode solution given in (19) into the difference equations in (16), we arrive at:

$$\begin{aligned}
1 &= z^{-1} + d_1(\kappa_1 - 2 + \kappa_1^{-1})(\theta + (1 - \theta)z^{-1}) \quad j < 0, \\
1 &= z^{-1} + 2d_1(-1 + \kappa_1^{-1})(\theta + z^{-1}(1 - \theta)) + 2rd_2z^{-1}(\kappa_2 - 1) \quad m = 1, j = 0, \\
1 &= z^{-1} + d_2(\kappa_2 - 2 + \kappa_2^{-1})(\theta + (1 - \theta)z^{-1}) \quad j > 0.
\end{aligned} \tag{20}$$

Solving the first and last equations for  $\kappa_1^{-1}$  and  $\kappa_2$  and substituting the two into the



second equation in (20), we obtain the equation for the amplification factor, i.e.  $z$ :

$$\sqrt{1 + \frac{4d_1(\theta(1 - z^{-1}) + z^{-1})}{1 - z^{-1}}} + \frac{rz^{-1}}{\theta(1 - z^{-1}) + z^{-1}} \left[ \sqrt{1 + \frac{4d_2(\theta(1 - z^{-1}) + z^{-1})}{1 - z^{-1}}} - 1 \right] = 0. \quad (21)$$

When the model problem is solved monolithically using the  $\theta$  scheme for time integration, it is unconditionally stable for large Fourier numbers ( $d_m \gg 1$ ). By considering the asymptotic solution to  $z$  under this assumptions, it is noted that for  $\theta = 0.5$ , the algorithm is unstable (see [5]). On the other hand, for Backward Euler ( $\theta = 1$ ), the algorithm is unconditionally stable. Since the loosely-coupled algorithm with  $\theta = 0.5$  is unstable for  $d_m \gg 1$ , it is of interest to obtain the point at which instability initiates. Following [6], (21) is solved for  $r$  and by substituting  $z = -1$  into the resultant equation, the value of  $r$  at which instability initiates is obtained:

$$r_s = \frac{(-1 + 2\theta)\sqrt{1 + 2d_1(1 - 2\theta)}}{-1 + \sqrt{1 + 2d_2(1 - 2\theta)}}. \quad (22)$$

It is observed that  $r_s(\theta = 0.5)$  is not defined. Using l' Hospital's Rule to evaluate the limit, we arrive at the following stability criterion for  $\theta = 0.5$ :

$$rd_2 < 1. \quad (23)$$

By substituting the definitions of  $r$  and  $d_2$  into the criterion, we obtain that

$$\frac{\Delta t \frac{k_2}{(\rho c_p)_1}}{\Delta x_1 \Delta x_2} < 1, \quad (24)$$

which imposes restriction on  $\Delta t$  given the material properties and grid size of the coupled domains.

## 5.1. Numerical results

In this section, the stability of the algorithm is investigated (with the explicit corrector step incorporated) by solving the model problem numerically. The results are compared to the analytical stability analysis. Each subdomain has a length of  $L_m = 0.5$ . The following initial condition is imposed on the global domain:  $T(x, t = 0) = 1, x \in \Omega_1$  and  $T(x, t = 0) = 0, x \in \Omega_2$ . The non-interface boundary conditions are set to  $T_1(x = -0.5) = 1$  and  $T_2(x = 0.5) = 0$ . Each subdomain is discretized using VFV method with  $N_m = 500$  ( $N_m$ : number of nodes in  $\Omega_m$ ). The materials of the coupled domains are varied according to Table 4 (see Table 3 for specifications of the material properties). The value of  $\theta$  is set to  $\theta = 0.5$ . The coupled problem is solved by integrating  $\Omega_1$  first (BGS-12). For each case,  $\Delta t$  is incremented until the computations become unstable. The *approximate*  $\Delta t$  and Fourier numbers  $d_m$  at which simulations become unstable are presented in Table 4.

For  $\theta = 0.5$ , it was derived (excluding the corrector step) that for stability  $rd_2 < 1$ . For all the three cases in Table 4, it is observed that instability initiates when this criterion is not satisfied. Therefore, (23) also provides a good estimate of the stability limit when the explicit corrector step is incorporated into the scheme.

Table 3. A list of properties of some materials.

Material	$\rho [\frac{kg}{m^3}]$	$c_p [\frac{J}{kg \cdot K}]$	$k [\frac{W}{m \cdot K}]$	$\alpha [\frac{m^2}{s}]$	$e [\frac{W \cdot s^{\frac{1}{2}}}{K \cdot m^2}]$
Steel	7500	500	48	$1.28 \cdot 10^{-5}$	$1.34 \cdot 10^4$
Water	1000	4800	0.6	$1.25 \cdot 10^{-7}$	1697.06
Air	1	1000	0.06	$6.0 \cdot 10^{-5}$	7.75

Table 4. Stability of the loosely-coupled algorithm with Crank-Nicolson for time integration.

case	$\sigma_{est}$	r	$d_1$	$d_2$	$\Delta t$	$rd_2$
steel-air	$5.8 \cdot 10^{-4}$	$2.7 \cdot 10^{-4}$	$8.0 \cdot 10^2$	$3.8 \cdot 10^3$	$6.3 \cdot 10^1$	1.0016
steel-water	$1.3 \cdot 10^{-1}$	$1.3 \cdot 10^0$	$8.0 \cdot 10^1$	$7.8 \cdot 10^{-1}$	$6.3 \cdot 10^0$	1.0016
steel-steel	$1 \cdot 10^0$	$1 \cdot 10^0$	$1.0 \cdot 10^0$	$1.0 \cdot 10^0$	$7.8 \cdot 10^{-2}$	1.0001

## 6. HIGHER ORDER IMEX SCHEMES

In this section, the model problem is advanced in time with the higher order multi-stage IMEX schemes presented in Section 4. We consider solving the coupled system, at each stage, integrating  $\Omega_1$  first (BGS-12). In computing the temperature field in  $\Omega_1$  at the implicit stage, denoted by  $(k)$ , application of the ESDIRK schemes to the semi-discrete equation of the interior cells, given by (9), results in:

$$(\rho c_p \Delta x)_1 T_{1,j}^{(k)} - (\rho c \Delta x)_1 T_{1,j}^n = \Delta t \sum_{i=1}^k a_{ki}^I (\mathcal{F}_{1,j})^{(i)}, j < 0 \quad (25)$$

where  $\mathcal{F}_{1,j}$  is defined in (9).

In computing the interface cell temperature  $T_{1,0}$  at the implicit stage of the ESDIRK schemes (the semi-discretized form of  $T_{1,0}$  is given in (10)), the explicit coupling term  $q_{1,0}$  is integrated with ERK schemes which are consistent with the applied ESDIRK schemes (the  $b_i$  and  $c_i$  coefficients of the two integration schemes are the same). In other words, the semi-discrete form of  $T_{1,0}$  is integrated in time using the higher order IMEX schemes. The discretization of  $T_{1,0}^{(k)}$  is given by:

$$\begin{aligned} (\rho c_p \frac{\Delta x}{2})_1 T_{1,0}^{(k)} - (\rho c_p \frac{\Delta x}{2})_1 T_{1,0}^n &= \Delta t \sum_{i=1}^k a_{ki}^I \left( -\frac{k_1}{\Delta x_1} (T_{1,0} - T_{1,-1}) \right)^{(i)} \\ &+ \Delta t \sum_{i=1}^{k-1} a_{ki}^E (-q_{1,0})^{(i)}. \end{aligned} \quad (26)$$

The solution to the time-level  $T_m^{n+1}$  is obtained by using (15) where through cancellation of the lower order error terms,  $T_m^{n+1}$  will retain its higher temporal accuracy.

### 6.1. Stability of IMEX schemes

In this section, the stability of the IMEX schemes is investigated by considering some numerical experiments. The results are compared to the conclusions of the stability analysis for the Crank-Nicolson scheme obtained earlier.

The same test case with the same parameters ( $L_m = .5$ ,  $N_m = 500$ ) as in Section 5.1 are used for the investigation. The third order IMEX (IMEX-3) scheme is used for time integration. For each case,  $\Delta t$  is incremented until the computations become unstable. The *approximate*  $\Delta t$  and Fourier numbers  $d_m$  at which simulations become unstable are presented in the table.

Table 5. Stability of the loosely-coupled algorithm with IMEX-3 for time integration.

case	$\sigma_{est}$	$\Delta x_1 = \Delta x_2$				$\Delta x_{2,C} = 0.5\Delta x_2$	$\Delta x_{1,C} = 0.5\Delta x_1$
		r	$d_1$	$d_2$	$\Delta t_{uni}$	$\frac{\Delta t_C}{\Delta t_{uni}}$	$\frac{\Delta t_C}{\Delta t_{uni}}$
steel-air	$5.8 \cdot 10^{-4}$	$2.7 \cdot 10^{-4}$	$6.5 \cdot 10^5$	$3.1 \cdot 10^6$	$5.1 \cdot 10^4$	1.8	1.8
steel-water	$1.3 \cdot 10^{-1}$	$1.3 \cdot 10^0$	$8.2 \cdot 10^2$	$8.0 \cdot 10^0$	$6.4 \cdot 10^1$	2.2	1.9
steel-steel	$1 \cdot 10^0$	$1 \cdot 10^0$	$3.8 \cdot 10^0$	$3.8 \cdot 10^0$	$3.0 \cdot 10^{-1}$	2.0	2.0

The results using the BGS-12 sequence are presented in Table 5. Similar results were obtained using BGS-21. Due to partly explicit nature of the IMEX scheme, it is expected that the loosely-coupled algorithm becomes unstable and as the results in the table indicate, instability occurs for all the cases considered.

In [5], it is reasoned that  $\sigma_{est}$  defined in (7) (the ratio between thermal effusivities of the domains) can be used as a measure of the physical strength of the coupling. Therefore, when  $\sigma_{est} \ll 1$ , the coupling is referred to as physically weak and as  $\sigma_{est} \rightarrow 1$  the strength of the coupling increases. For each case considered here, the corresponding values of  $\sigma_{est}$  obtained from (7), has also been included in the table. When the coupling between the domains is physically weak ( $\sigma_{est} \ll 1$ ), the IMEX schemes remain stable to large  $Fo$  numbers. However as  $\sigma_{est}$  approaches unity, the stability of the schemes reduces. By referring to the numerical results obtained for the Crank-Nicolson scheme (Table 4), a similar trend is observed. In addition, compared to the stability limit of the Crank-Nicolson scheme, the IMEX schemes demonstrate better stability properties, in particular for the case of *steel – air* coupling.

Based on the stability criterion for the Crank-Nicolson scheme, (24), the  $\Delta t$  for stability depends linearly on the mesh spacings  $\Delta x_m$ . To investigate if this relation also holds for the stability of the IMEX schemes, the grid in one domain is decreased by a factor of two (denoted as  $\Delta x_{m,C}$ ) while retaining the grid size fixed in the other. The last two columns of Table 5 imply that a linear relation appears to hold between  $\Delta t$  and  $\Delta x_m$ , as the approximate  $\Delta t$  at which instability initiates (denoted in the table by  $\Delta t_C$ ) is approximately twice as large as  $\Delta t_{uni}$ .

## 7. STABILITY OF THE STRONGLY-COUPLED ALGORITHM

It was observed in the previous section that as the thermal coupling between the domains becomes physically stronger, the stability (and temporal accuracy) of the loosely-coupled algorithm using the IMEX schemes for time integration reduces. Under such circumstances, it is more appropriate to use a strongly-coupled solution method where interface iterations are performed to stabilize and/or increase the temporal accuracy of the partitioned solution. In this section we study the stability and rate of convergence of performing (Gauss-Seidel) interface iterations at each stage of the higher order ESDIRK schemes in a strongly-coupled solution algorithm. The stability of the algorithm is analyzed for the model problem

described in Section 2. The analysis follows that of Henshaw and Chand [1] where the  $\theta$  scheme was used for time integration.

The problem is discretized in time but kept continuous in space. Application of the higher order ESDIRK schemes to (1) yields (noting that (2) is substituted for  $q_m$  in (1)):

$$T_m^{(k)}(x) - T_m^n(x) = \Delta t \alpha_m \sum_{i=1}^k a_{ki}^I \left( \frac{d^2 T_m}{dx^2} \right)^{(i)}, \quad \text{for } x \in \Omega_m, m = 1, 2 \quad (27)$$

where  $T_m^{(k)}(x) \approx T_m(x, t^{(k)})$  is the monolithic solution to the coupled problem, and  $t^{(k)} = t^n + c_k \Delta t$ . After some re-arrangements, the above equation can be written along with the corresponding boundary conditions as:

$$\frac{d^2 T_m^{(k)}}{dx^2} - \frac{1}{\Delta t a_{kk}^I \alpha_m} T_m^{(k)} = S_m, \quad \text{for } x \in \Omega_m, m = 1, 2 \quad (28)$$

$$T_2^{(k)}(\mathcal{I}) = T_1^{(k)}(\mathcal{I}), \quad (29)$$

$$k_1 \frac{dT_1^{(k)}}{dx} \Big|_{\mathcal{I}} = k_2 \frac{dT_2^{(k)}}{dx} \Big|_{\mathcal{I}}, \quad (30)$$

$$T_1^{(k)}(-L_1) = T_{1,lbc}, \quad T_2^{(k)}(L_2) = T_{2,rbc}, \quad (31)$$

where

$$S_m = \frac{-1}{\Delta t a_{kk}^I \alpha_m} \left[ T_m^n + \alpha_m \Delta t \sum_{i=1}^{k-1} a_{ki}^I \left( \frac{d^2 T_m}{dx^2} \right)^{(i)} \right], \quad \text{for } x \in \Omega_m, m = 1, 2 \quad (32)$$

are the known explicit contributions. The analysis is based on assuming that the previous solutions (to the time step or stage(s)) are equal to the exact solutions. In order to obtain the solution to the stage  $T_m^{(k)}$ , the implicit equations (28)-(31) need to be solved. Here, Block Gauss-Seidel iterations are considered to solve the equations. If we denote  $\{T_m^j\}_{j \geq 0}$  a sequence of iterates, we would like to see if the sequence converges to the monolithic solution, i.e.  $T_m^{(j)} \rightarrow T_m^{(k)}$  as  $j \rightarrow \infty$  starting from an initial guess. Following [1],  $\Omega_1$  is integrated first (BGS-12) in solving the coupled problem iteratively. Let us define the following iteration for  $j > 0$ :

$$\frac{d^2 T_m^{(j)}}{dx^2} - \frac{1}{\Delta t a_{kk}^I \alpha_m} T_m^{(j)} = S_m, \quad \text{for } x \in \Omega_m, m = 1, 2 \quad (33)$$

$$T_2^{(j)}(\mathcal{I}) = T_1^{(j)}(\mathcal{I}), \quad (34)$$

$$k_1 \frac{dT_1^{(j)}}{dx} \Big|_{\mathcal{I}} = k_2 \frac{dT_2^{(j-1)}}{dx} \Big|_{\mathcal{I}}, \quad (35)$$

$$T_1^{(j)}(-L_1) = T_{1,lbc}, \quad T_2^{(j)}(L_2) = T_{2,rbc}. \quad (36)$$

By subtracting out a particular solution to (28) and (31) that satisfies the homogeneous Dirichlet conditions at the interface, an iteration for the partitioning error  $\epsilon_m^{(j)}(x) = T_m^{(k)} - T_m^{(j)}$

is obtained:

$$\frac{d^2 \epsilon_m^{(j)}}{dx^2} = \beta_m^2 \epsilon_m^{(j)}, \quad \text{for } x \in \Omega_m, m = 1, 2 \quad (37)$$

$$\epsilon_2^{(j)}(\mathcal{I}) = \epsilon_1^{(j)}(\mathcal{I}) \quad (38)$$

$$k_1 \frac{d\epsilon_1^{(j)}}{dx} \Big|_{\mathcal{I}} = k_2 \frac{d\epsilon_2^{(j-1)}}{dx} \Big|_{\mathcal{I}} \quad (39)$$

$$\epsilon_1^{(j)}(-L_1) = 0, \epsilon_2^{(j)}(L_2) = 0 \quad (40)$$

with  $\beta_m$  defined as:

$$\beta_m = \sqrt{\frac{1}{a_{kk}^I \alpha_m \Delta t}}. \quad (41)$$

Carrying out the rest of the analysis following [1], we arrive at the equation for the amplification factor:

$$\mathcal{A} = -\frac{k_2 \beta_2 \tanh(\beta_1 L_1)}{k_1 \beta_1 \tanh(\beta_2 L_2)} = -\frac{k_2}{k_1} \sqrt{\frac{\alpha_1}{\alpha_2}} \frac{\tanh(\beta_1 L_1)}{\tanh(\beta_2 L_2)} \quad (42)$$

In [1], it is mentioned that in many cases  $\beta_1 L_1 \gg 1$  and  $\beta_2 L_2 \gg 1$  for which  $\tanh(\beta_1 L_1) \approx 1$  and  $\tanh(\beta_2 L_2) \approx 1$ . Under this assumption, the approximate rate of convergence of the iterations ( $|\mathcal{A}|$ ) is given by (7).

For the iterations to converge  $|\mathcal{A}| < 1$ , otherwise, as pointed out in Section 2, the imposed interface boundary conditions must be interchanged. It is observed that Dirichlet-Neumann formulation with Gauss-Seidel iterations will encounter difficulties when the subdomains have similar material properties  $|\mathcal{A}| \approx 1$  as opposed to  $|\mathcal{A}| \ll 1$  where the material properties of the two subdomains are far apart. For such cases ( $|\mathcal{A}| \approx 1$ ), methods to increase the rate of convergence of the iterations should be used, the simplest of which is the use of under-relaxation [1].

## 7.1. Numerical results

In this section, the model problem is solved numerically using the strongly-coupled algorithm for several cases (the material properties of the coupled domains are varied). For each case an average rate of convergence of iterations per stage of the ESDIRK,  $\sigma_{comp}^{(k)}$ , is computed and compared with the estimate  $\sigma_{est}^{(k)}$  obtained by performing stability analysis, (7). The same test case used for analyzing the stability of the IMEX schemes is considered with the following parameters: Each subdomain has a length of  $L_m = 0.1$  and is discretized using VEV method with  $N_m = 5000$ . The materials of the coupled domains are varied according to Table 6. The four-stage third order ESDIRK (ESDIRK-3) is used for time integration (note that the first stage is explicit). Computations are performed using  $\Delta t = 0.1$ . Following [1],  $\sigma_{comp}^{(k)}$  is obtained using:

$$\sigma_{comp}^{(k)} = \left( \frac{R^{(N)}}{R^{(1)}} \right)^{\frac{1}{N}}, \quad (43)$$

where for BGS-12, the residual is defined as  $R^{(j)} = |q_1(\mathcal{I})^{(j)} - q_1(\mathcal{I})^{(j-1)}|$ . Interface iterations are performed at each stage until  $R^{(N)} < 10^{-8}$ . To present the results in Table 6, for each stage,  $\sigma_{comp}^{(k)}$  is averaged over 10 time steps.

Table 6. Rate of convergence of interface iterations at each stage of ESDIRK-3

case	$\sigma_{comp}^{(k)}$			$\sigma_{est}^{(k)}$
	stage - 2	stage - 3	stage - 4	
steel-air	$5.7 \cdot 10^{-4}$	$5.7 \cdot 10^{-4}$	$5.7 \cdot 10^{-4}$	$5.8 \cdot 10^{-4}$
steel-water	$1.1 \cdot 10^{-1}$	$1.1 \cdot 10^{-1}$	$1.1 \cdot 10^{-1}$	$1.3 \cdot 10^{-1}$
steel-steel	$9.9 \cdot 10^{-1}$	$9.9 \cdot 10^{-1}$	$9.9 \cdot 10^{-1}$	$1 \cdot 10^0$

As the results show,  $\sigma_{est}^{(k)}$  provides a good estimate of the rate of convergence of subiterations for each stage of the ESDIRK. Furthermore, for each case, it is observed that  $\sigma_{comp}^{(k)}$  is almost the same for all stages. The main reason is the equality of the diagonal coefficients of the stages in the ESDIRK schemes.

## 8. CONCLUSIONS

Thermal interaction of fluids and solids, or conjugate heat transfer (CHT), is encountered in many engineering applications. Since time-accurate computations of such coupled problems can be computationally expensive, we considered loosely-coupled and strongly-coupled solution algorithms in which higher order multi-stage Runge-Kutta schemes were employed for time integration. The higher order time integration schemes have the potential to improve the computational efficiency at arriving at a certain accuracy relative to the traditionally used 1<sup>st</sup> and 2<sup>nd</sup> order implicit schemes. The spatial coupling between the subdomains was realized using Dirichlet-Neumann interface conditions and the coupled domains were solved in a sequential manner at each stage (Block Gauss-Seidel). The paper focused on the stability of two partitioned algorithms. A one dimensional model problem (which consists of two thermally coupled domains where the governing equation within each subdomain is unsteady linear heat conduction) was used for the stability analysis.

In the loosely-coupled approach, a family of higher order multi-stage mixed implicit-explicit (IMEX) Runge-Kutta schemes was used for time integration. The higher order IMEX schemes consist of the ESDIRK schemes for implicit integration of the spatially discretized governing equations within each subdomain and equal order and number of stages ERK schemes for explicit integration of all or part of the coupling terms. By observing similarities between the second stage of the IMEX schemes and the  $\theta$  scheme with  $\theta = 0.5$  (Crank-Nicolson), the stability of the partitioned algorithm in which the Crank-Nicolson scheme is used for time integration was first analyzed by applying the stability theory of Godunov-Ryabenkii. The stability of the IMEX schemes was next investigated by numerically solving the model problem. The results were compared to the conclusions of the stability analysis for the Crank-Nicolson scheme. Due to partly explicit nature of the IMEX schemes, the loosely-coupled algorithm becomes unstable for sufficiently large Fourier numbers (similar to the Crank-Nicolson scheme). When the ratio of the thermal effusivities of the coupled domains is much smaller than unity, time step restriction due to stability is sufficiently weak that computations can be performed with reasonably large Fourier numbers. Furthermore, the results showed better stability properties of the IMEX schemes compared to the Crank-Nicolson scheme. In addition, the results suggested that in the stability of the IMEX schemes, a linear relation appears to hold between time step size and the grid spacing of the domains, similar to what is observed in the stability criterion of the Crank-Nicolson scheme.

In the strongly-coupled approach, the stability and rate of convergence of performing (Gauss-Seidel) subiterations at each stage of the higher order implicit ESDIRK time integration schemes were analyzed. From the stability analysis, an expression for the rate of convergence of the iterations ( $\sigma$ ) was obtained. For cases where  $\sigma \ll 1$ , subiterations will converge rapidly. However, when  $\sigma \approx 1$ , the convergence rate of the iterations is slow. The results obtained by solving the model problem numerically were found to be in line with the performed analytical stability analysis.

## Acknowledgements

The financial support provided by Netherlands Technology Foundation STW is greatly appreciated.

## 9. REFERENCES

- [1] Henshaw W. D., Chand K. K., “A composite grid solver for conjugate heat transfer in fluid-structure systems”. *Journal of Computational Physics* 228, 3708-3741, 2009.
- [2] van Zuijlen A. H., Bijl H., “Implicit and explicit higher order time integration schemes for structural dynamics and fluid-structure interaction computations”. *Computers and Structures* 83, 93-105, 2005.
- [3] Giles M. B., “Stability analysis of numerical interface conditions in fluid-structure thermal analysis”. *Int. J. Numer. Meth. Fluids* 25, 421-436, 1997.
- [4] Kennedy C. A., Carpenter M. H., “Additive Runge-Kutta schemes for convection-diffusion-reaction equations”. *Applied Numerical Mathematics* 44, 139-181, 2003.
- [5] Kazemi-Kamyb V., van Zuijlen A. H., Bijl H., “Accuracy and stability analysis of a second order time-accurate loosely-coupled partitioned algorithm for transient conjugate heat transfer problems”. *Submitted to Comput. Methods Appl. Mech. Engrg*, 2011.
- [6] Roe B., Jaiman R., Haselbacher A., Geubelle P. H., “Combined interface boundary condition method for coupled thermal simulations”. *Int. J. Numer. Meth. Fluids* 57, 329-354, 2008.